ELSEVIER

Journal of Molecular Catalysis A: Chemical 187 (2002) 3–15

JOURNAL OF MOLECULAR CATALYSIS A: CHEMICAL

www.elsevier.com/locate/molcata

Oxidative catalysis by $Mn_4O_4^{6+}$ cubane complexes

Thomas G. Carrell, Shari Cohen, G. Charles Dismukes*

Department of Chemistry, Princeton University, Princeton, NJ 08544, USA

Received 22 October 2001; accepted 14 March 2002

Abstract

The oxidation of a variety of substrates (thioethers, hydrocarbons, alkenes, benyzl alcohol and benzaldehyde) by ^{t}BuOOH catalyzed by $Mn_4O_4(O_2PPh_2)_6$ (**1**) and $Mn_4O_4(O_2P(p\text{-MePh})_2)_6$ (**2**) is reported. These reactions illustrate the first examples of oxidative catalysis using a manganese-oxo complex with a Mn_4O_4 cubane core. These uncharged complexes contain Mn ions in a mixed valence oxidation state, formally Mn_4(2III, 2IV), and are bridged by bulky diphenylphosphinate chelates across each of the six faces of the cube. Using this system, methyl phenyl sulfide is selectively mono-oxygenated to methyl phenyl sulfoxide with high catalytic efficiency, and no evidence for further oxidation to the thermodynamically preferred sulfone. Toluene is oxidized to a mixture of benzyl alcohol, benzaldehyde, and benzoic acid with high catalytic efficiencies. Lower catalytic efficiencies are observed in the oxidation of styrene to a mixture of styrene oxide and benzaldehyde, of cyclohexene to a mixture of cyclohexene oxide, 2-cyclohexen-1-ol, and 2-cyclohexen-1-one, and of cyclohexane to a mixture of cyclohexanol and cyclohexanone. The observed product distribution from the oxidation of hydrocarbons has the characteristics of a free radical-based oxidation mechanism. However, the sulfoxidation and epoxidation activity of the **1**/^{t}BuOOH system, as well as the observed steric preferences for less congested substrates, suggest that a metal-oxo centered oxidation mechanism is active in the reactions studied here. An intermediate species, characterized by a UV–VIS band centered at 610 nm is observed in all reaction mixtures, and forms upon reaction of **1** or **2** with ^{t}BuOOH. Preliminary evidence suggests this reactive intermediate may correspond to a Mn(V)=O species. Kinetic studies suggest two pathways for oxidation: one involving an oxygen atom transfer (two-electron branch), and the other involving a hydrogen atom abstraction (one-electron branch).

Keywords: Oxidation; Polynuclear manganese complexes; Alkyl hydroperoxides

1. Introduction

The functionalization of inexpensive hydrocarbons to produce more valuable organic compounds such as alcohols, aldehydes, and ketones, requires the selective oxidation of strong C–H bonds. The development of catalysts that can perform these oxidations with adequate control of selectivity in an economically viable and environmentally friendly way represents one of the general goals of industrial, inorganic, and organometallic chemistry [1–3].

Manganese complexes have a long history in the oxidation of organic compounds. Potassium permanganate is widely used in the stoichiometric oxidation of a wide variety of compounds, including alkylbenzenes, alkenes, alcohols, and ketones [4]. Manganese porphyrin and Schiff base complexes are capable of performing a number of oxidations catalytically [5–7], sometimes even with high stereochemical selectivity [8–10], using a suitable oxidizing agent such as peroxides, iodosylbenzene, or even O_2. Mono- and polynuclear manganese complexes with non-macrocyclic

* Corresponding author. Tel.: +1-609-258-3949; fax: +1-609-258-1980.
E-mail address: dismukes@princeton.edu (G.C. Dismukes).

1381-1169/02/$ – see front matter
PII: S1381-1169(02)00139-5

ligands have also been effectively used as oxidation catalysts [11–15].

The relative energies of the manganese intermediates formed during the catalytic reaction cycle are a major determinant of the pathway of the oxidation reaction. When peroxides, such as hydrogen peroxide (H_2O_2) or alkyl hydroperoxides (ROOH), are used as the terminal oxidant, the manganese ion can cleave the peroxide O–O bond either heterolytically or homolytically. Heterolytic cleavage by a Mn(III) complex usually results in the formation of a high-valent Mn(V)=O complex, which occurs with certain strong-field macrocyclic ligands [16–20]. The manganese-oxo group is a very strong oxidant, yet can perform highly selective oxidations that depend on the choice of substrate and its accessibility to the Mn=O moiety. Applications to selective oxidations have been reported [5,8–10,17,21]. Alternatively, homolytic cleavage of the peroxide O–O bond leads to the generation of free radicals (either $HO^{\bullet}$ or $RO^{\bullet}$). These radicals, also being very strong oxidants, react with organic substrates with little or no selectivity [1]. The choice of which of these pathways and catalyst systems to choose obviously depends on the task at hand. The determination of the mechanism that occurs in a catalytic oxidation reaction is not always straightforward. The Gif [22–24] and Fenton [25–27] oxidation systems are two examples of well-studied systems in which the mechanism of substrate oxidation has been difficult to discern.

Previously, we described the syntheses of the manganese-oxo complex $Mn_4O_4(O_2PPh_2)_6$ (**1**) [28] and the isostructural derivative $Mn_4O_4(O_2P(p\text{-}MePh)_2)_6$ (**2**) [29]. Both contain the $Mn_4O_4^{6+}$ cubane core with an average manganese oxidation state of +3.5 (Fig. 1). These complexes react stoichiometrically with secondary organoamines ($RR'NH$) to form 4 equiv. of the amino radical, the "pinned-butterfly" complex, $Mn_4O_2(O_2PPh_2)_6$, and release two core oxos as H_2O molecules [30]. The cubanes **1** and **2** also undergo efficient photo-rearrangement in the gas phase to produce O_2 by intramolecular elimination of two corner oxo atoms in a reaction that requires the release of one phosphinate ligand, forming the "open-butterfly" complex $[Mn_4O_2(O_2PPh_2)_5]^+$ [29,31].

Herein, we extend the range of chemistries of these cubane clusters by examining their utility as oxidation catalysts, using ^{t}BuOOH as the terminal oxidant.

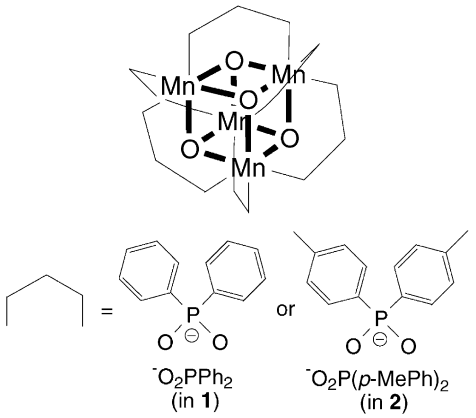

Fig. 1. Molecular representation of the catalysts used in this study. Catalysts **1** and **2** differ only by a methyl group in the *para*-position of the phenyl moiety in the diphenylphosphinate ligand.

Initial evidence for a mechanism of substrate oxidation in these reactions is presented.

2. Experimental

2.1. Materials

All solvents and reagents purchased from commercial sources, were of the highest available purity, and were used without further purification. De-oxygenated CH_2Cl_2 for anaerobic trials was prepared by distillation from CaH_2 under an Ar atmosphere. De-oxygenated toluene and cyclohexane for anaerobic trials was prepared by vigorous bubbling with Ar for at least 3 h prior to use. Catalyst **2** [29] was prepared as described elsewhere. Purity was assessed by FT-IR and NMR.

2.2. Synthesis of *1*

HO_2PPh_2 (3.0 mmol, 0.66 g) and NaOH (3.0 mmol, 0.12 g) are dissolved in 35 ml of DMF. $Mn(ClO_4)_2 \cdot 6H_2O$ (1.4 mmol, 0.51 g) is dissolved in 15 ml of DMF and is added with stirring to the NaO_2PPh_2 solution. A light-brown solution forms in a few minutes. $KMnO_4$ (0.6 mmol, 0.10 g) is dissolved in 35 ml of DMF, and is added dropwise with stirring to the reaction mixture with stirring, immediately forming a maroon solution. The reaction mixture is stirred for 3 h, producing a red precipitate of **1**, which is washed using three 25 ml

portions of CH_3OH followed by three 25 ml portions of Et_2O. The precipitate is then dried in air to produce analytically pure **1**. Yield: 0.56 g (71%).

2.3. Instrumentation

^1H NMR spectra were collected as $CDCl_3$ solutions on either a JEOL 270 MHz spectrometer or a GE-300 MHz spectrometer. UV–VIS spectra were measured on an HP-8452A spectrophotometer using quartz cuvettes with a 1.0 cm path length. FT-IR spectra were measured on a Nicolet 730 FT-IR spectrometer as KBr pellets.

2.4. General catalytic reaction conditions

An aliquot of the substrate (methyl phenyl sulfide: 2.6×10^{-3} mol, 0.30 ml, 1040 equiv.; styrene: 2.6×10^{-3} mol, 0.30 ml, 1040 equiv.; cyclohexene: 3.0×10^{-3} mol, 0.20 ml, 1200 equiv.; benzyl alcohol: 2.4×10^{-3} mol, 0.25 ml, 960 equiv.; benzaldehyde: 2.5×10^{-3} mol, 0.25 ml, 1000 equiv.) was dissolved in 10 ml of a 0.25 mM solution of **1** (2.5×10^{-6} mol) in CH_2Cl_2. The catalytic oxidation reaction was then initiated by the addition of an aliquot of ^{t}BuOOH. The reaction mixtures were stirred until bleaching of the red-orange color from **1** was complete. The solution was then passed over a silica column to remove the Mn products. Characterization of the organic products was performed using ^1H NMR in $CDCl_3$. An aliquot of dioxane was added as an internal standard for quantitative determination of yields. All reactions were carried out without thermostating at ambient temperature.

Anaerobic reactions were performed using common Schlenk techniques under an atmosphere of Ar [32]. All solvents and reagents were degassed immediately prior to use as described under Section 2.1. Upon completion of the reaction, the work-up procedure was performed aerobically using the method described above.

2.5. Reaction conditions for the oxidation of hydrocarbons

An amount of 3.5 mg of **2** (2.0×10^{-6} mol) was dissolved in 10 ml of toluene. An aliquot of ^{t}BuOOH was then added to initiate the reaction. The solution was stirred until the bleaching of the red-orange color of **2** was complete. The reaction mixture was then subjected to the work-up described above. Reactions involving cyclohexane were performed in a similar fashion using cyclohexane as the solvent, except a small amount of CH_2Cl_2 (0.5 ml) was added to the reaction mixture to ensure the complete dissolution of **2**.

2.6. General considerations

All of the reported data represent an average from a minimum of three trials. In all cases, the standard deviation from the mean was <10% of the reported value. Identical control experiments in which either the catalyst (**1** or **2**) or ^{t}BuOOH was omitted from the reaction mixture resulted in no reaction in all cases.

2.7. Kinetic measurements

Reactions were monitored by UV–VIS spectrophotometry from 190 to 820 nm at room temperature. The catalyst concentration (**1** or **2**) was 0.10 mM in all reactions. Three types of reactions were studied. (1) Methyl phenyl sulfide (25 μl, 0.10 M) was added to 2.0 ml of 0.10 mM **1** in CH_2Cl_2. An aliquot of ^{t}BuOOH was added, and spectra were recorded in 15 s intervals. (2) **2** was prepared as a 0.10 mM solution in toluene. An aliquot of ^{t}BuOOH was added to 2.0 ml of this solution, and spectra were recorded in 5 min intervals. (3) A control experiment was performed in which an aliquot of ^{t}BuOOH was added to 2.0 ml of a 0.10 mM solution of **1** in CH_2Cl_2. Spectra were recorded in 2 min intervals.

3. Results

The ability of the **1**/^{t}BuOOH system to catalyze the sulfoxidation of thioethers was examined using methyl phenyl sulfide as a model substrate in large excess (>1000-fold with respect to the catalyst **1**). Only methyl phenyl sulfoxide is observed as an oxidation product in these reactions with no evidence for further oxidation to methyl phenyl sulfone (Scheme 1), even though the formation of the sulfone from the sulfoxide is thermodynamically more favorable than the formation of the sulfoxide from the thioether [33]. This result is comparable to other catalytic thioether oxidation systems [34,35]. At low concentrations

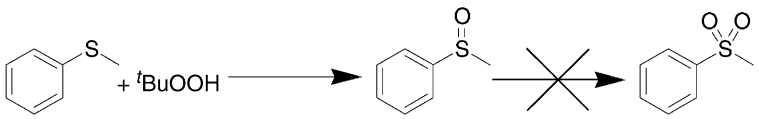

Scheme 1.

of ^{t}BuOOH (6.9 mM, 28 equiv. with respect to **1**; Table 1, Entry 1), catalytic efficiencies (defined as the yield of oxidized products with respect to the terminal oxidant ^{t}BuOOH) as high as 94% are observed. At higher ^{t}BuOOH concentrations, the catalytic efficiency decreases to approximately 60% (Table 1, Entry 2). This corresponds to 56 catalytic turnovers (defined as the ratio of the moles of product to the moles of catalyst **1**) at a ^{t}BuOOH concentration of 23 mM (98 equiv. with respect to **1**). When the same reaction is performed under an Ar atmosphere using degassed CH_2Cl_2, the yield of methyl phenyl sulfoxide is unchanged relative to the aerobic reaction in the same period of time (Table 1, Entry 3). Therefore, we conclude that the oxygen atom of the sulfoxide derives exclusively from the catalyst/oxidant system.

The oxidation of alkenes by the **1**/^{t}BuOOH system was also examined using two model substrates in large excess (>1000-fold over **1**): styrene and cyclohexene. The oxidation of styrene under these conditions produces a mixture of styrene oxide and benzaldehyde (Scheme 2) in an approximately 1:2 ratio (Table 1, Entries 4 and 5). The reaction proceeds with a relatively low catalytic efficiency of approximately 20%. When O_2 is excluded from the reaction mixture, the product distribution changes dramatically and the number of turnovers decreases by 1/3, so that styrene oxide is formed as the major product (83% of the total yield) with benzaldehyde making up the remaining 17% of the yield (Table 1, Entry 6). In addition, the color from **1** does not completely bleach in 5 h of reaction time when O_2 is excluded from the solution,

Table 1
Results from the oxidation of thioethers and alkenes by ^{t}BuOOH catalyzed by **1**

Entry[a]	Substrate[b]	[^{t}BuOOH] (mM) (equiv.)	Product (yield[c], %)	Catalytic efficiency[d] (%)	TON[e]	Time (h)
1	Me–S–Ph	6.9 (28)	Me–S(O)–Ph (100)	94	26	10[f]
2	Me–S–Ph	23 (98)	Me–S(O)–Ph (100)	60	56	25[f]
3	Me–S–Ph (anaerobic)	23 (98)	Me–S(O)–Ph (100)	59	52	30[f]
4	Styrene	11 (44)	Styrene oxide (37) Benzaldehyde (63)	20	9	2.5
5	Styrene	22 (88)	Styrene oxide (35) Benzaldehyde (65)	13	12	2.5
6	Styrene (anaerobic)	11 (44)	Styrene oxide (83) Benzaldehyde (17)	14	6	5
7	Cyclohexene	11 (44)	2-Cyclohexen-1-ol (46) 2-Cyclohexen-1-one (51) Cyclohexene oxide (3)	46	20	1.5
8	Cyclohexene	22 (88)	2-Cyclohexen-1-ol (44) 2-Cyclohexen-1-one (52) Cyclohexene oxide (4)	24	21	1.5
9	Cyclohexene (anaerobic)	22 (88)	No reaction		0	3

[a] Reactions were performed with 0.25 mM **1** in CH_2Cl_2.
[b] [Me–S–Ph] = 0.26 M; [styrene] = 0.25 M; [cyclohexene] = 0.30 M.
[c] Fraction of the yield of a given product compared to the total yield of products.
[d] Total moles of product relative to the moles of added ^{t}BuOOH.
[e] Total moles of product relative to the moles of catalyst **1**.
[f] These values are in minutes.

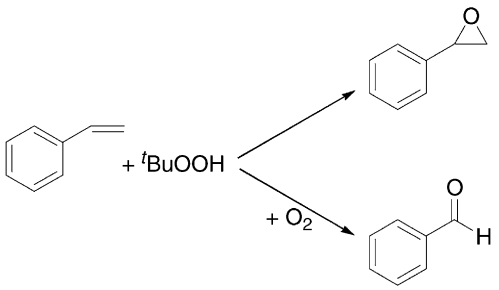

Scheme 2.

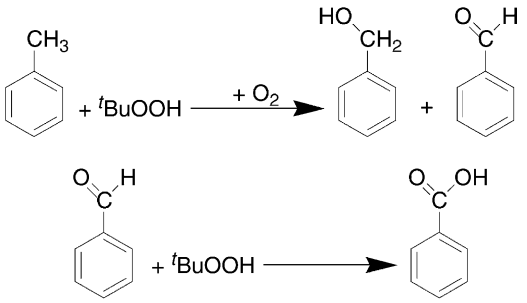

Scheme 4.

whereas aerobic reactions show complete bleaching of **1** in 2.5 h. The catalytic efficiency remains low in the absence of O_2 (14% efficiency with 11 mM ^{t}BuOOH). These results suggest that two different pathways for the oxidation of styrene are present. One pathway leads to the epoxidation of styrene to form styrene oxide, and is not dependent on O_2, whereas the second pathway leads to the formation of benzaldehyde and is dependent on O_2. When the reaction is performed in air, both pathways are active, producing the observed 1:2 ratio of styrene oxide to benzaldehyde. However, in the absence of O_2, styrene oxide continues to form by the O_2 independent pathway while the formation of benzaldehyde in inhibited.

The oxidation of cyclohexene by the **1**/^{t}BuOOH system also produces a mixture of products (Table 1, Entries 7 and 8). The major products are 2-cyclohexen-1-ol and 2-cyclohexen-1-one (Scheme 3), which are produced in almost equal yields. Cyclohexene oxide is formed as a minor product (3% yield based on the total yield of oxidized products). The catalytic efficiency is higher for the oxidation of cyclohexene (46% efficiency with 11 mM ^{t}BuOOH) than is observed for the oxidation of styrene. Reactions performed anaerobically show no evidence for the formation of any oxidized products from cyclohexene, indicating an absolute requirement for O_2 (Table 1, Entry 9). The product distribution is characteristic of hydrogen atom abstraction at the β-position of cyclohexene to form an allyl radical intermediate, rather than oxygen atom transfer, which would result in epoxidation at the C=C bond. The low epoxidation yield suggests that the decreased stereochemical accessibility of the cyclohexene C=C bond relative to the styrene C=C bond may be responsible for the faster allylic oxidation over epoxidation in cyclohexene.

The possibility of oxidizing primary alkyl substituents attached to an aromatic framework was examined by studying the reaction of **2** and ^{t}BuOOH in toluene. The cubane derivative **2** exhibits greater solubility in toluene than does **1**, so that reactions could be performed directly in toluene without the need for additional solvent (e.g. CH_2Cl_2) to ensure dissolution of the catalyst. The addition of ^{t}BuOOH to a toluene solution of **2** (0.20 mM) results in the formation of benzyl alcohol and benzaldehyde as the major products, representing approximately 80% of the total yield, with benzoic acid making up the remainder (Scheme 4). Catalytic efficiencies of 165% are observed with a ^{t}BuOOH concentration of 11 mM (Table 2, Entry 10). The efficiency decreases with higher concentrations of ^{t}BuOOH, resulting in 95% catalytic efficiency and 101 turnovers with respect to **2** with a ^{t}BuOOH concentration of 22 mM. When these reactions are performed under anaerobic conditions, the yield of oxidized products plummets, with only 8 turnovers in 3 h and a catalytic efficiency of 14% (Table 2, Entry 12).

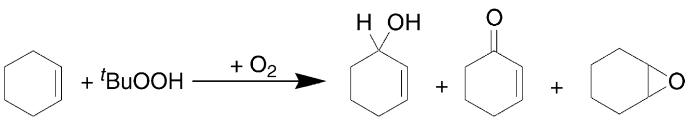

Scheme 3.

Table 2
Results from the oxidation of hydrocarbons and related compounds by ^{t}BuOOH catalyzed by **2** (or **1**)

Entry	Substrate[a]	[^{t}BuOOH] (mM) (equiv.)	Product (yield[b], %)	Catalytic efficiency[c] (%)	TON[d]	Time (h)
10[e]	Toluene	11 (55)	Benzyl alcohol (36) Benzaldehyde (45) Benzoic acid (19)	165	91	3
11[e]	Toluene	22 (110)	Benzyl alcohol (41) Benzaldehyde (41) Benzoic acid (18)	95	101	3
12[e]	Toluene (anaerobic)	11 (55)	Benzyl alcohol (47) Benzaldehyde (53)	14	8	3
13[f]	Benzyl alcohol	22 (88)	Benzaldehyde (100)	11	9	2
14[f]	Benzaldehyde	22 (88)	Benzoic acid (100)	175	154	1
15[e]	Cyclohexane	22 (110)	Cyclohexanol (55) Cyclohexanone (45)	6	7	2.5
16	Cyclohexane (anaerobic)	22 (110)	No reaction		0	2.5

[a] [Benzyl alcohol] = 0.24 M; [benzaldehyde] = 0.25 M.
[b] Fraction of the yield of a given product compared to the total yield of products.
[c] Total moles of product relative to the moles of added ^{t}BuOOH.
[d] Total moles of product relative to the moles of catalyst **1**.
[e] Reactions were performed with [**2**] = 0.20 mM.
[f] Reactions were performed with [**1**] = 0.25 mM.

The formation of benzyl alcohol and benzaldehyde in approximately equal proportions from toluene is consistent with an O_2-dependent free radical reaction pathway known as the Russell reactions (Fig. 2) [36]. This mechanism, when applied to the oxidation of toluene, involves an initial hydrogen atom abstraction from the methyl group to form the benzyl radical, Ph–$CH_2^\bullet$, which subsequently adds O_2, followed by disproportionation of the peroxyl radical to form equal amounts of the corresponding alcohol and aldehyde. The nearly equivalent yields of benzyl alcohol and benzaldehyde from the **2**/^{t}BuOOH oxidation system suggests the presence of this mechanism, which is further supported by the significant reduction in the yield of oxidized products when the reactions are performed in the absence of O_2. The observation of catalytic efficiencies that exceed 100% at a ^{t}BuOOH concentration of 11 mM also suggests an O_2-dependent auto-oxidation pathway. We have attempted to trap the proposed Ph–$CH_2^\bullet$ radical intermediate in this pathway using $CBrCl_3$, a known alkyl radical trap [37], but were unsuccessful due to a rapid reaction between $CBrCl_3$ and **2**.

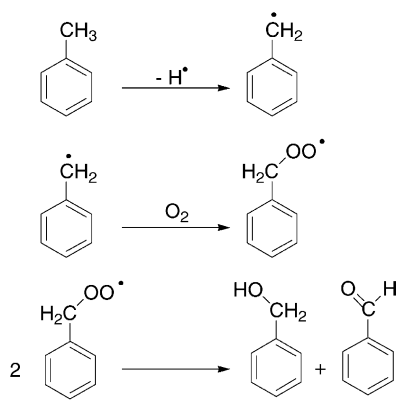

Fig. 2. The Russell reaction pathway, as applied to the oxidation of toluene. This pathway involves the initial hydrogen atom abstraction from toluene followed by subsequent reactions involving O_2.

To further test the proposed Russell reaction pathway in the oxidation of toluene by **2**/^{t}BuOOH, we also examined the reactivity of the **1**/^{t}BuOOH system towards benzyl alcohol in CH_2Cl_2 (Table 2, Entry 13). Benzaldehyde is the only product formed under these reaction conditions, however the yield is approximately five times lower than is observed in the oxidation of toluene by **2**/^{t}BuOOH (11% catalytic efficiency with respect to 22 mM ^{t}BuOOH). The low yield supports the hypothesis that benzyl alcohol and benzaldehyde are formed concomitantly in

pure toluene by the Russell reactions. However, the Russell pathway only accounts for the formation of benzyl alcohol and benzaldehyde from the oxidation of toluene, and does not directly account for the formation of benzoic acid (Table 2, Entries 10 and 11).

The oxidation of benzaldehyde by the **1**/^{t}BuOOH system in CH_2Cl_2 was therefore examined to determine if this reaction could be the source of the observed benzoic acid. Benzoic acid is the only observed product in the reaction of **1**/^{t}BuOOH with benzaldehyde, producing high yields over a short period of time (175% catalytic efficiency, 154 turnovers in 1 h; Table 2, Entry 14). Thus, the low catalytic efficiency for formation of benzoic acid from toluene by **2**/^{t}BuOOH (Table 2) is consistent with formation by subsequent oxidation of free benzaldehyde that is initially formed free in solution by the Russell pathway. Although, benzaldehyde is oxidized quickly and in high yield using CH_2Cl_2 solvent, this reaction must compete with oxidation of toluene and thus is greatly suppressed using toluene as solvent. This competition is presumed to account for the retention of the approximately 1:1 product ratio of benzaldehyde to benzyl alcohol required by the Russell pathway.

Finally, the activity of the **2**/^{t}BuOOH system towards secondary aliphatic C–H bonds was examined using cyclohexane as a substrate and the solvent. Cyclohexane is oxidized to produce a mixture of cyclohexanol and cyclohexanone in nearly equal proportions under aerobic reaction conditions (Scheme 5). However, the catalytic efficiencies are much lower (6% efficiency with respect to 22 mM ^{t}BuOOH) than are observed for the oxidation of toluene under similar conditions (Table 2, Entry 15). The formation of an equimolar amount of cyclohexanol and cyclohexanone from cyclohexane is commonly attributed to the Russell reactions resulting from an initial hydrogen atom abstraction from cyclohexane [37,38]. The requirement for O_2 that is an integral part of the Russell reactions is further supported by the absence of any oxidized products when the reaction is performed anaerobically (Table 2, Entry 16).

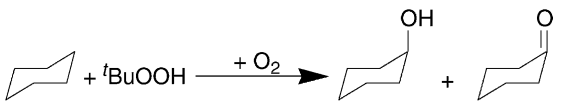

Scheme 5.

In each of the reactions described above, the catalyst (either **1** or **2**) is completely bleached, forming a cloudy white solution/suspension, indicative of reduction to a Mn(II) material. This reduction process occurs via reaction of the substrate with an oxidized precursor that forms between the ^{t}BuOOH and the catalyst. Initial attempts to identify this species are described next.

Three representative reactions were monitored by UV–VIS spectrophotometry: the reaction of ^{t}BuOOH with **1** in CH_2Cl_2 in the presence of a large excess of methyl phenyl sulfide (Fig. 3a), the reaction of

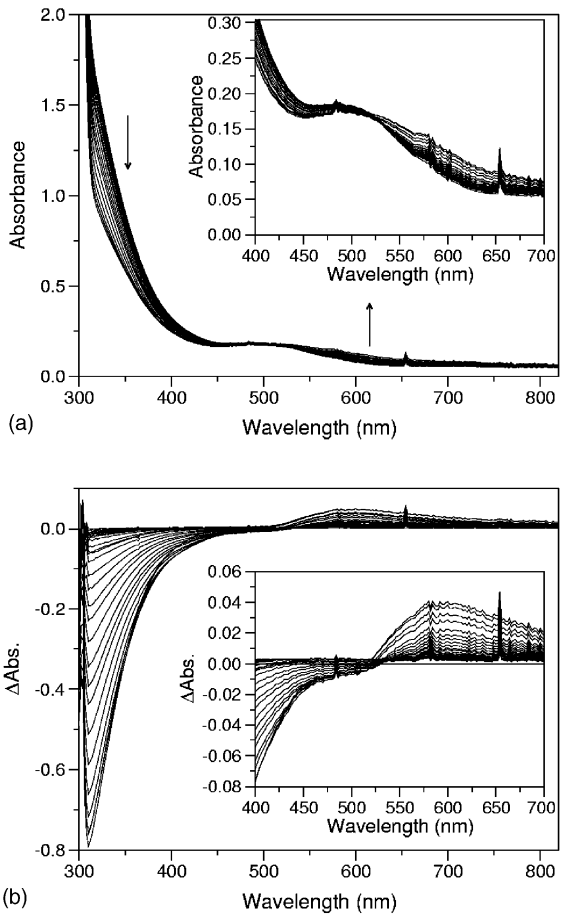

Fig. 3. (a) Spectral changes during the reaction of methyl phenyl sulfide (0.10 M) with **1** (0.10 mM) and ^{t}BuOOH (2.8 mM) in CH_2Cl_2, measured in 15 s intervals. (b) Difference spectra, referenced to the spectrum recorded at $t = 0$ min. Inset (for both the parts): enlargement of the region between 400 and 700 nm.

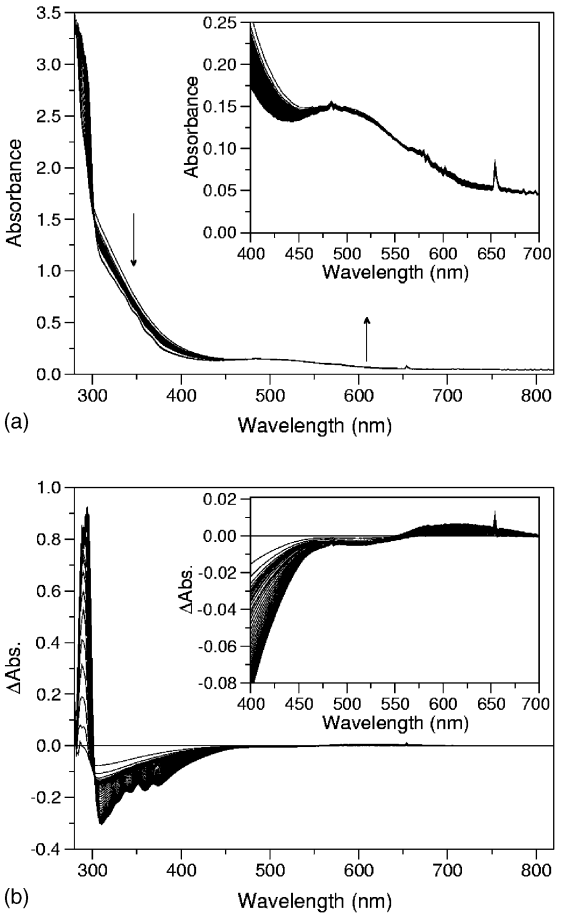

Fig. 4. (a) Spectral changes during the reaction of ^{t}BuOOH (2.8 mM) with **2** (0.10 mM) in toluene, measured in 5 min intervals. (b) Difference spectra, referenced to the spectrum recorded at $t = 0$ min. Inset (for both the parts): enlargement of the region between 400 and 700 nm.

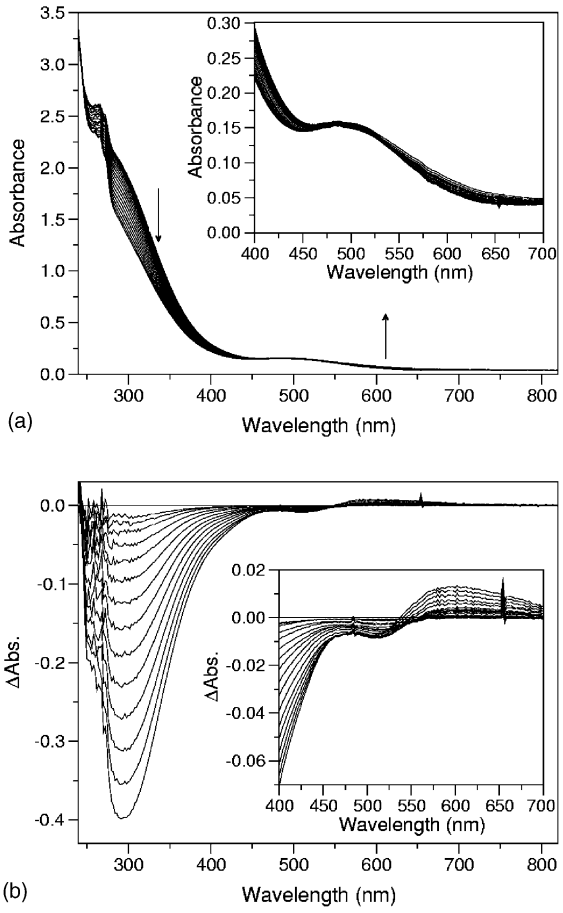

Fig. 5. (a) Spectral changes during the reaction of ^{t}BuOOH (2.8 mM) with **1** (0.10 mM) in CH_2Cl_2, measured in 2 min intervals. (b) Difference spectra, referenced to the spectrum recorded at $t = 0$ min. Inset (for both the parts): enlargement of the region between 400 and 700 nm.

^{t}BuOOH with **2** in toluene (Fig. 4a), and the reaction of ^{t}BuOOH with **1** in CH_2Cl_2 in the absence of an oxidizable substrate (Fig. 5a). Similar spectral features are observed in these three reactions, which can be seen more easily by plotting difference spectra relative to the spectrum measured at $t = 0$ min (Figs. 3b, 4b and 5b). All three reactions produce a negative peak at approximately 300 nm in the difference spectra, as well as a positive peak at approximately 610 nm. An isosbestic point is observed at 535 nm in the presence of methyl phenyl sulfide for the first 5 min of the reaction. This isosbestic point is shifted to 560 nm when the reaction of **2** and ^{t}BuOOH is performed in toluene, as well as in the reaction of **1** and ^{t}BuOOH in the absence of a substrate in CH_2Cl_2. These isosbestic points persist for 180 and 20 min, respectively, in these reactions. The similarity of the spectral changes in all three reactions suggests that a common reactive intermediate forms between the catalyst complex (**1** or **2**) and ^{t}BuOOH that does not require the substrate.

The UV–VIS spectral changes described above exhibit three kinetically resolved phases. The solutions are optically clear during the three resolved phases, but the reactions typically end by turning cloudy due to the formation of a white precipitate, which masks the final phase of the reaction. The rate and duration of these

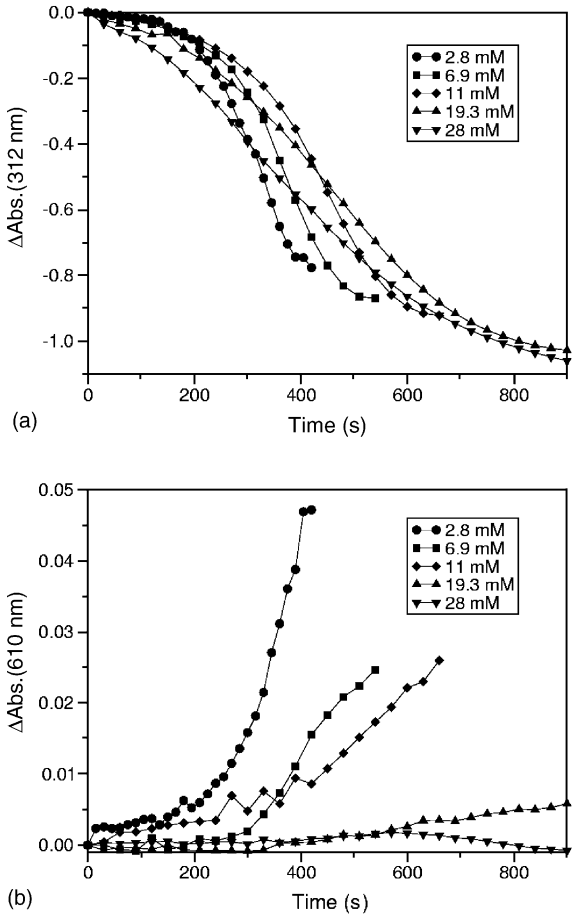

Fig. 6. Change in the absorbance at (a) 312 nm and (b) 610 nm during the reaction of methyl phenyl sulfide (0.10 M) with **1** (0.10 mM) and ^{t}BuOOH (2.8 mM) in CH_2Cl_2.

phases depend on both the ^{t}BuOOH concentration and the identity of the substrate (or lack thereof). The presence of multiple phases differs from that expected for a simple bimolecular reaction and suggests the formation of an intermediate prior to product formation.

The reaction of ^{t}BuOOH and **1** in the presence of methyl phenyl sulfide in CH_2Cl_2 produces the most rapid reaction measured (Fig. 6). The absorbance change at 312 nm (Fig. 6a) exhibits an initial slow or lag phase in which there is minimal bleaching, followed by a faster phase of constant bleaching that eventually slows in the third phase, signaling the end of the reaction. Cloudiness appears due to a white colloidal material in the latter stages of the termination phase. The duration of the initial lag phase is extended as the concentration of ^{t}BuOOH is increased from 2.8 to 11 mM, but decreases from 19.3 to 28 mM. By contrast, the slope of the second phase remains constant from 2.8 to 11 mM, but progressively slows down as this concentration is increased above 11 mM, so that the transition between the first two phases is blurred at higher ^{t}BuOOH concentrations. The change in absorbance at 610 nm (Fig. 6b) also reflects these three phases in terms of rate and duration, although the second and third phases are not well resolved at this wavelength.

The reaction between ^{t}BuOOH and **1** in CH_2Cl_2 in the absence of an oxidizable substrate also exhibits three kinetic phases, however the rates are approximately five times slower than when methyl phenyl

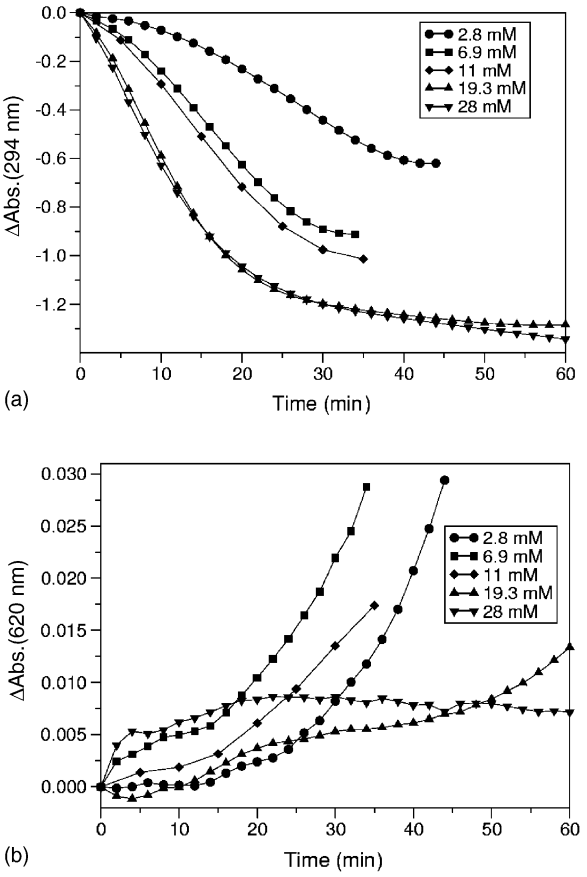

Fig. 7. Change in the absorbance at (a) 294 nm and (b) 620 nm during the reaction of ^{t}BuOOH (2.8 mM) with **1** (0.10 mM) in CH_2Cl_2.

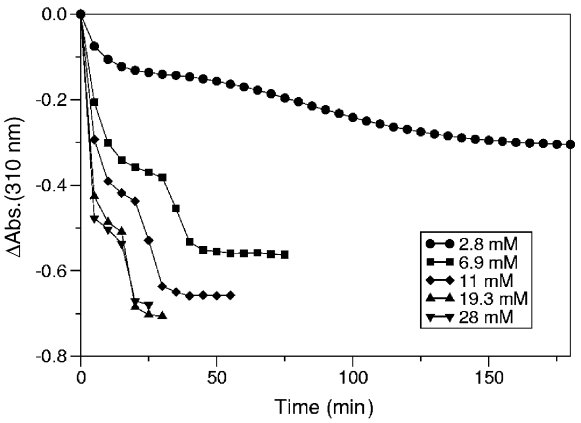

Fig. 8. Change in the absorbance at 310 nm during the reaction of ^{t}BuOOH (2.8 mM) with **2** (0.10 mM) in toluene.

sulfide is present in solution (Fig. 7). As the concentration of ^{t}BuOOH is increased from 2.8 to 19.3 mM, the duration of the lag phase shortens and the slope of the second phase accelerates. At ^{t}BuOOH concentrations of 19.3–28 mM, the kinetics exhibit no dependence on the initial concentration of ^{t}BuOOH.

On the other hand, the kinetic behavior is fundamentally different in the reaction of **2** and ^{t}BuOOH in toluene. This reaction exhibits four kinetic phases, alternating between fast and slow (Fig. 8). All four phases speed up as the concentration of ^{t}BuOOH is increased from 2.8 to 19.3 mM, but become independent of the initial ^{t}BuOOH concentration between 19.3 and 28 mM.

4. Discussion

The manganese-oxo cubanes **1** and **2** have the ability to catalyze the oxidation of a wide variety of organic compounds using ^{t}BuOOH as a terminal oxidant. Both oxygen atom transfer (sulfoxidation and epoxidation) and hydrogen atom abstraction have been observed.

Any complete mechanistic interpretation of these results requires consideration of the two main pathways in which the O–O bond of the terminal oxidant ^{t}BuOOH can be cleaved upon reaction with the catalyst (Fig. 9). ^{t}BuOOH typically reacts with a metal complex to form an initial metal-alkylperoxo intermediate (M^{n+}–OOR; Fig. 9, reaction (a)). The O–O bond of the coordinated peroxide can then cleave heterolytically to form a high-valent metal-oxo complex ($M^{(n+2)+}$=O) and ^{t}BuOH (Fig. 9, reaction (b)), or homolytically to form ^{t}BuO$^\bullet$ radicals and a metal hydroxide complex ($M^{(n+1)+}$–OH; Fig. 9, reaction (c)).

In the catalytic oxidation of hydrocarbons, the observation of the Russell reactions (Fig. 2) leading to the formation of approximately equal yields of alcohol and ketone is usually interpreted as evidence that freely diffusing radicals are formed in the initial oxidation step by hydrogen atom abstraction [37]. The hydrogen atom abstractor in this pathway is usually thought to be a free radical species (i.e. ^{t}BuO$^\bullet$), since it is expected that hydrogen atom abstraction by a metal-based species (either M=O or M–OOR) will result in almost exclusive alcohol formation due to the rapid recombination of the oxidant and substrate radical ("oxygen-rebound" mechanism) [37]. On this basis, the simplest interpretation of the product yields observed for oxidation of toluene, cyclohexane, and cyclohexene is that a free radical oxidant such as ^{t}BuO$^\bullet$ is active in the **1** (or **2**)/^{t}BuOOH system.

However, the complexity of the kinetics of the spectral changes suggest that the reaction that leads to substrate oxidation is more complex than just a simple bimolecular reaction between **1** and ^{t}BuOOH to produce ^{t}BuO$^\bullet$ radicals. Additionally, the rate of product

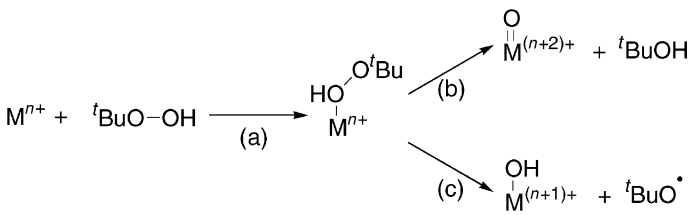

Fig. 9. Three possible pathways for the cleavage of the O–O bond of ^{t}BuOOH: (a) heterolytic cleavage, leading to the formation of a high-valent M=O moiety; (b) simple binding of ^{t}BuOOH to form a Mn–OO^{t}Bu complex; (c) homolytic cleavage, leading to the formation of ^{t}BuO$^\bullet$ radicals.

formation exhibits a marked dependence on the substrate identity. The reaction in which methyl phenyl sulfide is oxidized to methyl phenyl sulfoxide is especially curious, since the duration of the lag phase increases initially with increasing ^{t}BuOOH concentration and the rate of the second phase slows down as the ^{t}BuOOH concentration is increased further (Fig. 6). The kinetics are consistent with the formation of an initial intermediate between ^{t}BuOOH and **1** (Fig. 10, reaction (a)), which then can either

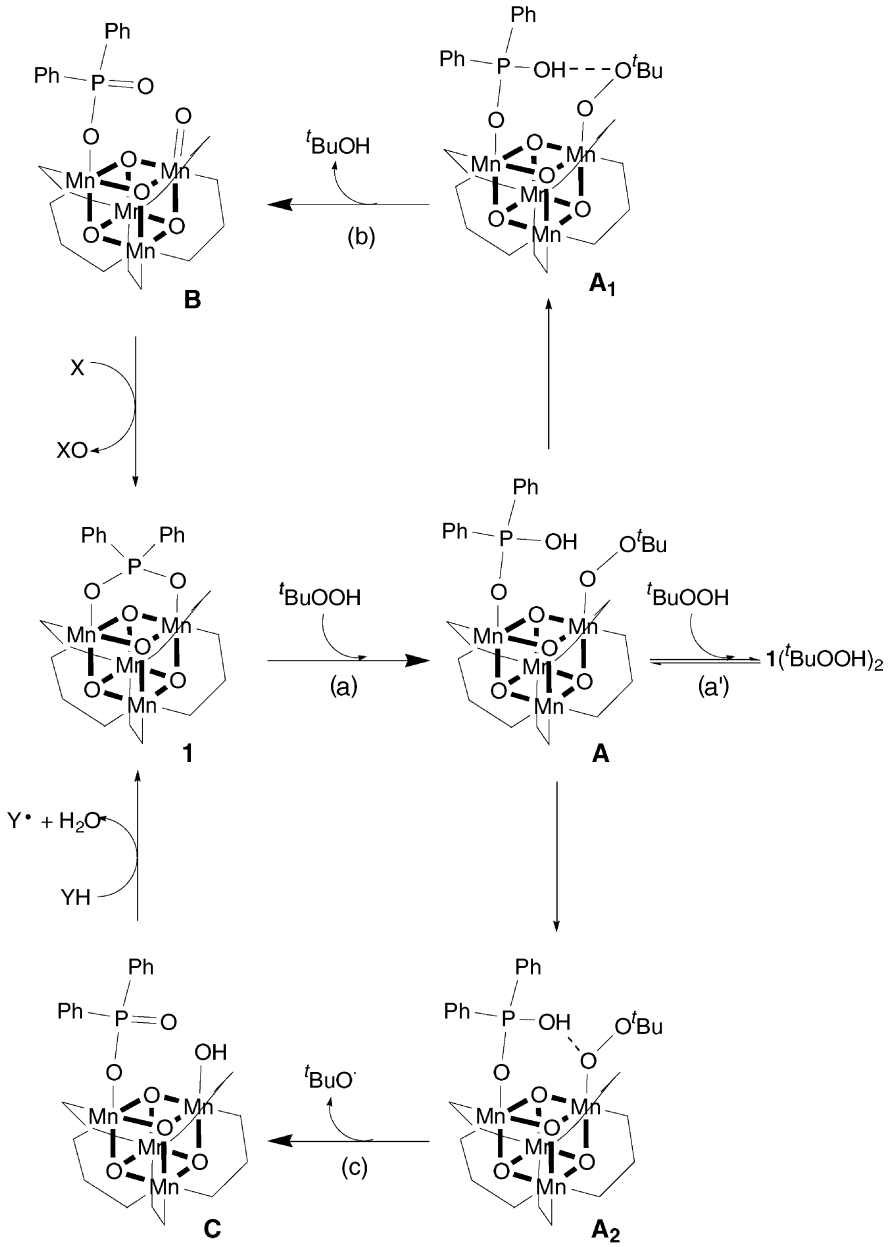

Fig. 10. Proposed reaction cycle for oxidation reactions involving ^{t}BuOOH catalyzed by the manganese-oxo cubanes **1** and **2**. For clarity, only one chelating diphenylphosphinate ligand is shown in the cluster.

be reduced by reaction with the substrate (312 nm bleaching) or be blocked from reduction by reacting with excess ^{t}BuOOH (Fig. 10, reaction (a′)). The latter reaction, if reversible, would retard the rate of reaction with the substrate and extend the lifetime of the initial intermediate (i.e. extend the lag phase).

A reaction scheme that is consistent with our experimental observations is shown in Fig. 10. The initial binding of ^{t}BuOOH to **1** (reaction (a)) would result in the transfer of a proton to a phosphinate ligand, forming a complex that could resemble intermediate **A** in Fig. 10. Intramolecular hydrogen bonding between the coordinated phosphinic acid and ^{t}BuOO$^-$ is stereochemically permitted and thermodynamically expected in the non-polar solvent (CH_2Cl_2 or toluene). This could involve either the distal or proximal O atoms of ^{t}BuOO$^-$, as suggested by structures $\mathbf{A}_1$ and $\mathbf{A}_2$, respectively. Heterolytic O–O bond cleavage would be facilitated by the hydrogen bonding by proton transfer from the phosphinic acid to the distal O atom (intermediate $\mathbf{A}_1$), resulting in the release of ^{t}BuOH (reaction (b)). Considerations of electron count would require that the intermediate correspond to a formal oxidation state of Mn(V)=O, and might resemble the six-coordinate species shown as intermediate **B** in Fig. 10. Mn(V)=O species are known to be active oxidants in many porphyrin catalyst systems [16–19]. This "two-electron" pathway could account for some of the observed substrate oxidation, here suggested to correspond to oxygen atom transfer ($X + B \rightarrow XO$). On the other hand, proton transfer to the proximal O atom (intermediate $\mathbf{A}_2$) should result in homolytic O–O bond cleavage, releasing ^{t}BuO$^\bullet$ radicals and forming a Mn(IV)–OH species, intermediate C (reaction (c)). This "one-electron" pathway might also account for some of the observed substrate oxidation, here suggested to correspond to a hydrogen atom abstraction pathway ($YH + C \rightarrow Y + H_2O$). Since a free radical pathway involving ^{t}BuO$^\bullet$ radicals can also account for the observed oxygen atom transfer products, it is not possible to state that either a Mn(V)=O or ^{t}BuO$^\bullet$ radical oxidant is active in the **1** (or **2**)/^{t}BuOOH catalytic system, exclusively.

Intermediate **B** may be the species that is observed in the UV–VIS spectrum of the reaction mixture. This species is characterized by a band that appears at approximately 610 nm, and is only dependent on the catalyst **1** or **2** and ^{t}BuOOH, but not on the substrate. The shift in the broad absorbance band at 500 nm to longer wavelengths upon reaction of **1** or **2** with ^{t}BuOOH is consistent with the formation of a Mn=O complex. The replacement of a phosphinate oxygen donor ligand (O^-–P^+R_3) to Mn by an oxide ligand (O^{2-}) is expected to produce a substantial shift to lower energies of the O → Mn charge transfer bands involving the phosphinate ligands, which occur in this region of the spectrum based on electronic assignments [39,40]. Similar bands have been observed at around 550–650 nm in several high-valent Mn=O complexes [17,21,41,42].

Acknowledgements

We thank Dr. P. Baesjou for helpful discussions in the early phases of this work. We also thank Prof. J.T. Groves for useful comments in the preparation of this manuscript. Financial support from the National Institutes of Health (Grant GM-39932) is appreciated.

References

[1] R.A. Sheldon, J.A. Kochi, Metal-Catalyzed Oxidation of Organic Compounds, Academic Press, New York, 1981.
[2] G.W. Parshall, S.D. Ittel, Homogeneous Catalysis, 2nd Edition, Wiley, New York, 1992.
[3] A.E. Shilov, G.B. Shul'pin, Chem. Rev. 97 (1997) 2879–2932.
[4] J. March, Advanced Organic Chemistry: Reactions, Mechanisms, and Structure, 4th Edition, Wiley, New York, 1992.
[5] B. Meunier, Chem. Rev. 92 (1992) 1411–1456.
[6] R.A. Sheldon (Ed.), Metalloporphyrins in Catalytic Oxidations, Marcel Dekker, New York, 1994.
[7] T. Katsuki, Coord. Chem. Rev. 140 (1995) 189–214.
[8] W. Zhang, J.L. Loebach, S.R. Wilson, E.N. Jacobsen, J. Am. Chem. Soc. 112 (1990) 2801–2803.
[9] R. Irie, K. Noda, Y. Ito, N. Matsumoto, T. Katsuki, Tetrahedron Asym. 2 (1991) 481–494.
[10] M. Palucki, N.S. Finney, P.J. Pospisil, M.L. Güler, T. Ishida, E.N. Jacobsen, J. Am. Chem. Soc. 120 (1998) 948–954.
[11] R.H. Fish, R.H. Fong, J.B. Vincent, G. Christou, J. Chem. Soc., Chem. Commun. (1988) 1504–1506.
[12] J.E. Sarneski, D. Michos, H.H. Thorp, M. Didiuk, T. Poon, J. Blewitt, G.W. Brudvig, R.H. Crabtree, Tetrahedron Lett. 32 (1991) 1153–1156.
[13] T. Matsushita, D.T. Sawyer, A. Sobkowiak, J. Mol. Catal. A: Chem. 137 (1999) 127–133.
[14] G.B. Shul'pin, G. Süss-Fink, L.S. Shul'pina, J. Mol. Catal. A: Chem. 170 (2001) 17–34.

[15] S.A. Chavan, S.B. Halligudi, D. Srinivas, P. Ratnasamy, J. Mol. Catal. A: Chem. 161 (2000) 49–64.
[16] N. Jin, J.T. Groves, J. Am. Chem. Soc. 121 (1999) 2923–2924.
[17] J.T. Groves, J. Lee, S.S. Marla, J. Am. Chem. Soc. 119 (1997) 6269–6273.
[18] K. Wietzerbin, J.G. Muller, R.A. Jameton, G. Pratviel, J. Bernadou, B. Meunier, C.J. Burrows, Inorg. Chem. 38 (1999) 4123–4127.
[19] J. Bernadou, B. Meunier, Chem. Commun. (1998) 2167–2173.
[20] C.G. Miller, S.W. Gordon-Wylie, C.P. Horwitz, S.A. Strazisar, D.K. Peraino, G.R. Clark, S.T. Weintraub, T.J. Collins, J. Am. Chem. Soc. 120 (1998) 11540–11541.
[21] Z. Gross, G. Golubkov, L. Simkhovich, Angew. Chem. Int. Ed. Engl. 39 (2000) 4045–4047.
[22] D.H.R. Barton, D. Doller, Acc. Chem. Res. 25 (1992) 504–512.
[23] R. Çelenligil-Çetin, R.J. Staples, P. Stavropoulos, Inorg. Chem. 39 (2000) 5838–5846.
[24] S.B. Marr, R.O. Carvel, D.T. Richens, H.-J. Lee, M. Lane, P. Stavropoulos, Inorg. Chem. 39 (2000) 4630–4638.
[25] C. Walling, Acc. Chem. Res. 8 (1975) 125–131.
[26] C. Walling, Acc. Chem. Res. 31 (1998) 155–157.
[27] P.A. MacFaul, D.D.M. Wayner, K.U. Ingold, Acc. Chem. Res. 31 (1998) 159–162.
[28] W.F. Ruettinger, C. Campana, G.C. Dismukes, J. Am. Chem. Soc. 119 (1997) 6670–6671.
[29] M. Yagi, K. Wolfe, P. Baesjou, S. Bernasek, G.C. Dismukes, Angew. Chem. Int. Ed. Engl. 40 (2001) 2925–2928.
[30] W.F. Ruettinger, G.C. Dismukes, Inorg. Chem. 39 (2000) 1021–1027; erratum (2000) 1039, 4186.
[31] W.F. Ruettinger, M. Yagi, K. Wolfe, S. Bernasek, G.C. Dismukes, J. Am. Chem. Soc. 122 (2000) 10353–10357.
[32] D.F. Shriver, M.A. Drezdzon, The Manipulation of Air Sensitive Compounds, 2nd Edition, Wiley/Interscience, New York, 1986.
[33] R.H. Holm, J.P. Donahue, Polyhedron 12 (1993) 571–589.
[34] C. Duboc-Toia, S. Ménage, R.Y.N. Ho, L. Que Jr., C. Lambeaux, M. Fontecave, Inorg. Chem. 38 (1999) 1261–1268.
[35] S. Mukerjee, K. Skogerson, S. DeGala, J.P. Caradonna, Inorg. Chim. Acta 297 (2000) 313–329.
[36] G.A. Russell, J. Am. Chem. Soc. 79 (1957) 3871–3877.
[37] P.A. MacFaul, K.U. Ingold, D.D.M. Wayner, L. Que Jr., J. Am. Chem. Soc. 119 (1997) 10594–10598.
[38] J. Kim, C. Kim, R.G. Harrison, E.C. Wilkinson, L. Que Jr., J. Mol. Catal. A: Chem. 117 (1997) 83–89.
[39] D.R. Gamelin, M.L. Kirk, T.L. Stemmler, S. Pal, W.H. Armstrong, J.E. Penner-Hahn, E.I. Solomon, J. Am. Chem. Soc. 116 (1994) 2392–2399.
[40] M. Yagi, D. McClure, G.C. Dismukes, Unpublished work.
[41] H. Sakiyama, H. Okawa, R. Isobe, J. Chem. Soc., Chem. Commun. (1993) 882–884.
[42] F.M. MacDonnell, N.L.P. Fackler, C. Stern, T.V. O'Halloran, J. Am. Chem. Soc. 116 (1994) 7431–7432.